SINGULAR RISE AND SINGULAR DROP OF CUTOFF FREQUENCIES IN SLOT LINE AND STRIP LINE WAVEGUIDES

C.Y. Wang

Departments of Mathematics and Mechanical Engineering, Michigan State University, East Lansing, MI 48824, USA

ABSTRACT

The complete frequency spectrum of the circularly- shielded slot line and strip line are determined using an efficient domain decomposition and mode matching method. Asymptotic analyses show that, when the gap width of the slot line or the width of the strip line are too small, the TE frequencies may drop singularly and the TM frequencies may rise singularly. These new properties greatly affect the cutoff frequencies.

KEYWORDS

waveguide, singular behavior, slot line, strip line,TM and TE

1. INTRODUCTION

Due to their favorable bandwidth separation and compactness in size, waveguides with slot lines and strip lines have become important in many microwave and millimeter wave applications (Collin 1960, Edwards 1992, Gupta et al 1996). Longitudinal strips protruding from the wall include fin lines or slot lines (Bhat and Koul 1987, Tsalamengas et al 1993). Longitudinal strips that are suspended inside a waveguide are called strip lines (Omar and Schunemann 1989, Babili et al 1992). Because of their complicated geometries, these structures are difficult to analyze theoretically and a variety of numerical method were used, with various degrees of success.

The slot line in an elliptic guide was considered by El-Sherbiny (1973), who used Mathieu functions and separation of variables. He suggested that the fundamental TE frequency may drop to zero when the slot becomes to narrow. Tsalamengas et al (1993) using singular integral equations computed several TM and TE frequencies for the slot line in a waveguide also noted such a trend. On the other hand, the strip line suspended inside a waveguide was considered by Babili et al (1992) using singular integrals and Ragheb and Hassan (2004) using Mathieu functions, but they did not discover any sharp rise or drop in frequency, since small strip widths were not considered. Thus the properties of the circularly shielded slot line or strip line are still incomplete.

In this paper we are interested in the properties of the basic slot line and strip line in a circular metallic waveguide, especially establishing the singular rise or singular drop in frequencies when the width changes. As we shall see later, such singular behavior is important in the design of waveguide structures.

We shall use the semi-analytic mode-matching method complemented by a an asymptotic method in the singular regions. In comparison to the method of singular integrals and the method of Mathieu functions used by previous authors, the mode-matching method is more efficient and more accurate especially near the singular regions. Since all numerical methods fail at the singularities, rigorous asymptotic analyses will be used to explore the nature of the singularity and thus complete the frequency spectrum.

The assumptions (and limitations) are as follows.

1) The circular shield, with the extended fins or strip insert are perfectly conducting.
2) The cross section of the waveguide does not vary longitudinally.
3) Material properties such as permeability and permittivity are constant.
4) The filling inside the waveguide is empty or loss-less.
5) The small amplitude electromagnetic waves are linear.

1. THE SLOT LINE IN A CIRCULAR WAVEGUIDE

Fig.1a shows the cross section of the waveguide where the cylinder radius is *R* and two vertical fins of length *bR* protrude from the wall. The slot is of width 2(1-*b*)*R*. For both TM (transverse magnetic) and TE (transverse electric) modes the governing Helmholtz equation in cylindrical coordinates (r,θ) is

$$\frac{\partial^2 w}{\partial r^2}+\frac{1}{r}\frac{\partial w}{\partial r}+\frac{1}{r^2}\frac{\partial^2 w}{\partial \theta^2}+k^2 w=0 \qquad (1)$$

Here *w* is the scalar wave amplitude function, all lengths are normalized by *R*, and the eigenvalue or normalized frequency is

$$k=2\pi R f(\mu_0\varepsilon_0)^{1/2} \qquad (2)$$

In Eq.(2) *f* is the frequency, μ_0 is the free-space permeability, and ε_0 is the free-space permittivity. For the TM modes, the boundary condition is that *w* is zero on all surfaces, and for the TE modes the normal derivative of *w* is zero.

We shall use the method of mode matching which is most suited for these problems. Fig.1b shows a representative quadrant in cylindrical coordinates (r,θ) partitioned into two regions. Let the subscript I denote the inner region $r < b$, $0\le\theta\le\pi/2$ and the subscript II denote the outer region $b\le r\le 1$, $0\le\theta\le\pi/2$. The outer region is bounded by one protruding fin. Eigenfunction expansions that satisfy partial boundary conditions are constructed for each region,

and they are matched for continuity at their common boundary at *r*=1-*b*. For nontrivial solutions, the normalized frequency is found from the resulting characteristic equation.

We classify the mode shapes by their symmetry properties. If the mode is symmetric with respect to both vertical and horizontal directions, it is designated by the subscript SS. If the mode is symmetric vertically (about $\theta = 0$) and anti-symmetric horizontally (about $\theta = \pi/2$) it is designated by SA. If the mode is anti-symmetric vertically and symmetric horizontally it is designated by AS. If the mode is anti-symmetric both vertically and horizontally it is designated by AA.

Consider first the TM mode, which is related to the vibrating membrane. If it is ymmetric both horizontally and vertically, the mode is TMSS. For Region I the general solution to Eq.(1) which is bounded and has zero derivatives both $\theta = 0$ and $\theta = \pi/2$ is

$$w_I = \sum_{n=0}^{\infty} A_n \cos(2n\theta) J_{2n}(kr) \tag{3}$$

The general solution to Region II, which is zero on *r* =1, symmetric at $\theta = 0$ and zero at $\theta = \pi/2$ is

$$w_{II} = \sum_{n=1}^{\infty} B_n \cos[(2n-1)\theta] H_{2n-1}(kr) \tag{4}$$

Where

$$H_\beta(kr) = Y_\beta(k) J_\beta(kr) - J_\beta(k) Y_\beta(kr) \tag{5}$$

Here in Eq.(5) *J* and *Y* are Bessel functions of first and second kinds. Truncate the series in Eq.(4) to *N* terms each and take *N* evenly-spaced collocation points on the first quadrant arc along *r*=1-*b*. The angles are given by Eq.(6)

$$\theta_j = \frac{(j-0.5)\pi}{2N}, \quad j = 1 \text{ to } N \tag{6}$$

At their common boundary at *r* =1- *b*, continuity of the amplitude and its normal derivative for the two regions require

$$\sum_{n=0}^{N-1} A_n \cos(2n\theta_j) J_{2n}[k(1-b)] = \sum_{n=1}^{N} B_n \cos[(2n-1)\theta_j] H_{2n-1}[k(1-b)] \tag{7}$$

$$\sum_{n=0}^{N-1} A_n \cos(2n\theta_j) J_{2n}'[k(1-b)] = \sum_{n=1}^{N} B_n \cos[(2n-1)\theta_j] H_{2n-1}'[k(1-b)] \tag{8}$$

where the prime denote derivative with respect to *r*. Eqs.(7,8) constitute a set of 2*N* homogeneous algebraic equations. For nontrivial solutions the determinant of the coefficients of *A* and *B* is set to zero, giving the eigenvalue *k*. Usually a three-figure accuracy is attained when the number of terms retained *N* is increased to about 30. The lowest TM wave number (the cutoff eigenvalue) is of importance and is shown in Table 1.

Table 1 The first (cutoff) TM frequency (TMSS) as a function of fin length *b*

b	0	0.1	0.2	0.3	0.4	0.5	0.6	0.7	0.8	0.9	1.
k	2.405	2.415	2.455	2.528	2.640	2.800	3.018	3.290	3.571	3.768	3.832

For the TMSA mode the fin lies on the vertical symmetry line and have no effect. The solution is Eq.(9)

$$w = \cos[(2n-1)\theta]J_{2n-1}(kr) \tag{9}$$

The eigenvalues are the roots of $J_{2n-1}(k) = 0$ or *k*= 3.8317, 6.3802, 7.1056, etc.

For the TMAS mode the partial solutions for Regions I and II are

$$w_I = \sum_{n=1}^{\infty} A_n \sin[(2n-1)\theta]J_{2n-1}(kr) \tag{10}$$

$$w_{II} = \sum_{n=1}^{\infty} B_n \sin(2n\theta)H_{2n}(kr) \tag{11}$$

A similar point match of Eqs.(10,11) on *r*=1-*b* yields the normalized frequency *k*.

For the TMAA case again the fin does not affect the mode. The solution is Eq.(12)

$$w = \sin(2n\theta)J_{2n}(kr) \tag{12}$$

The frequencies are *k*= 5.1356, 7.5883, 8.4172, etc.

The first TE mode is TESA. The Region I solution has the same form as Eq.(9) but the Region II solution is

$$w_{II} = \sum_{n=0}^{\infty} B_n \cos(2n\theta)K_{2n}(kr) \tag{13}$$

In Eq.(13)

$$K_\beta(kr) = Y_\beta'(k)J_\beta(kr) - J_\beta'(k)Y_\beta(kr), \tag{14}$$

The primes in Eq.(14) denote differentiation with respect to r. The first TE (cutoff) frequency is of importance and is tabulated in Table 2. Notice the sudden drop in frequency from *b*=0.9 to 1, or for very narrow slots. This property will be investigated more closely later.

Table 2 The first (cutoff) TE frequency (TESA) as a function of fin length *b*

B	0	0.1	0.2	0.3	0.4	0.5	0.6	0.7	0.8	0.9	1.
K	1.841	1.831	1.798	1.737	1.644	1.525	1.390	1.248	1.098	0.928	0

For the TEAS mode the solution is Eq.(15)

$$w = \sin[(2n-1)\theta]J_{2n-1}(kr) \tag{15}$$

The frequencies are the zeros of $J_{2n-1}'(k) = 0$ or *k*= 1.8412, 4.2012, 5.3314, etc

For the TEAA mode the Region I solution has the same form as Eq.(12) and that for Region II is given in Eq.(16)

$$w_{II} = \sum_{n=1}^{\infty} B_n \sin[(2n-1)\theta]K_{2n-1}(kr) \tag{16}$$

For the TESS mode the fins have no effect. The solution is Eq.(17)

$$w = \cos(2n\theta)J_{2n}(kr) \tag{17}$$

where $J_0'(k) = 0$ or *k*= 3.0542, 3.8317, 5.3176, etc.

The change in both TM and TE frequencies are plotted in Fig. 2. These curves agree qualitatively with the graphs of Tsalamengas et al (1993). Table 3 shows a comparison with Chen et al (2005), who did not consider the extreme fin lengths.

Table 3 Comparison of (cutoff) TM frequency (TMSS) as a function of fin length.
Asterisked values are from Chen et al (2005)

b	0	0.2	0.4	0.6	0.8	1
k	2.405	2.455	2.640	3.018	3.571	3.832
	- -	2.45*	2.63*	3.04*	3.56*	- -

2. THE STRIP LINE IN A CIRCULAR WAVEGUIDE

Fig. 2(c) shows a shielded strip line. We divide the quadrant into two Regions as shown in Fig. 2(d). For the TMss Mode the solution can be written as Eqs.(18,19)

$$w_I = \sum_{n=1}^{\infty} A_n \cos[(2n-1)\theta]J_{2n-1}(kr) \tag{18}$$

$$w_{II} = \sum_{n=0}^{\infty} B_n \cos(2n\theta)H_{2n}(kr) \tag{19}$$

where H is defined in Eq.(5). Similar point match yields the frequencies. Table 4 shows the first TM frequency.

Table 4 The first (cutoff) TM frequency (TMSS) as a function of strip length 2b

B	0	0.1	0.2	0.3	0.4	0.5	0.6	0.7	0.8	0.9	1.
K	2.405	3.060	3.296	3.496	3.653	3.753	3.803	3.824	3.830	3.832	3.832

Table 4 agrees to three digits with the numerical results of Yu and Wang (2001) who studied the fundamental frequency of a membrane constrained by a strip. Notice the sharp rise in frequency from b=0 to b=0.1.

For the TMSA mode the strip does not affect the solution which is Eq.(9). The frequencies are also same.

For the TMAS mode Region I is represented by Eq.(12) while Region II has the form Eq. (20)

$$w_{II} = \sum_{n=1}^{\infty} B_n \sin[(2n-1)\theta] H_{2n-1}(kr) \tag{20}$$

For the TMAA mode the strip does not affect the solution which is Eq.(12). The frequencies are also same.

The first TE frequency is TESA. The solutions are represented by Eqs.(21,22)

$$w_I = \sum_{n=0}^{\infty} A_n \cos(2n\theta) J_{2n}(kr) \tag{21}$$

$$w_{II} = \sum_{n=1}^{\infty} B_n \cos[(2n-1)\theta] K_{2n-1}(kr) \tag{22}$$

Table 5 shows the numerical values of this cutoff frequency.

Table 5 The first (cutoff) TE frequency (TESA) as a function of strip length 2b

b	0	0.1	0.2	0.3	0.4	0.5	0.6	0.7	0.8	0.9	1.
k	1.841	1.821	1.762	1.667	1.548	1.417	1.284	1.152	1.016	0.861	0

Again we note the sharp drop to zero for b close to one.

The TEAS mode, for which the strip has no effect, is given by Eq.(15) with its corresponding frequencies.

The TEAA mode is described by Eq.(10) and for Region II Eq.(23)

$$w_{II} = \sum_{n=1}^{\infty} B_n \sin(2n\theta) K_{2n}(kr) \tag{23}$$

The TESS mode is not affected by the strip and is given by Eq.(17). The corresponding frequencies are same.

Fig. 3 shows our computed TM and TE frequencies as the strip width is varied. Notice there is a sharp rise in cutoff TMSS frequency for small *b*, and a sharp drop for all the varying TE frequencies when *b* is close to one. Babili et al (1992) found the sharp rise in cutoff TM mode but did not detect the sharp drop in the TE modes.

Fig. 4 shows a comparison of our results with those of Babili et al (1992) whose used the singular integral equation method. The two sources agree perfectly but diverges for $b>0.8$. Typical convergence rates for our mode matching method is shown in Table 6.

Table 6. Typical convergence rate when the number of terms N retained is increased. (TM modes for strip line).

N	*b*=0.4 1st mode	*b*=0.4 3rd mode	*b*=0.3 1st mode
5	3.627	4.473	3.469
10	3.642	4.505	3.485
15	3.648	4.516	3.491
20	3.650	4.522	3.494
23	3.652	4.525	3.495
30	3.653	4.527	3.496
35	3.653	4.529	3.497
40		4.529	3.497

Table 7 shows a comparison with the limited existing numerical results.

Table 7. Comparison of TM frequency with various sources

source	present	Yu and Wang (2001)	Chen et al (2005)	Lee and Chen (2012)
method	mode match	mode match	fundamental solution	boundary element
b=0.4 1st	3.653	3.655	3.65	3.677
b=0.4 3rd	4.529	- -	4.52	4.514
b=0.3 1st	3.496	3.498	3.502	- -

3. ASYMPTOTIC ANALYSIS

Consider first the sharp rise in the cutoff TMSS frequency for a small strip (Fig.3). For the TM mode, $w=0$ on the strip is similar to a small constraint at the center. The problem is analogous to the vibration of circular membrane with a small centered constraint. The following analysis is a brief description from Wang (1998) who studied the problem of a vibrating membrane with a small circular core of normalized radius *b*. Using Rayleigh's exact axisymmetric solution (1945)

given by Eq.(24)

$$w = J_0(k)Y_0(kr) - Y_0(k)J_0(kr) \tag{24}$$

The characteristic equation is Eq.(25)

$$J_0(k)Y_0(kb) - Y_0(k)J_0(kb) = 0 \tag{25}$$

For small *b*, let the frequency be perturbed from the no-core value k_0

$$k = k_0 + \delta(b)k_1 + o(\delta) \tag{26}$$

where $\delta(b)$ is a guage function. The expansion of Eq.(25) for small *b* then yields the gauge function Eq.(27)

$$\delta(b) = \frac{1}{|\ln(b)|} \tag{27}$$

We expect the asymptotic behavior for a small strip also has such inverse-log singularity. Using the numerical data {*b*,*k*} from mode matching, i.e. {0.1, 3.060},{0.05, 2.917}, {0.333, 2.858} Eq.(26) is written as

$$k_1 = (k - k_0)|\ln b| \tag{28}$$

Here k_0 =2.4048, the TM cutoff value for the circular waveguide without the strip. From Eq.(28) and the data, the constant k_1 is approximately 1.54. Thus the asymptotic formula is

$$k = 2.4048 + \frac{1.54}{|\ln b|} + \cdots \tag{29}$$

Eq.(29) is shown as the dotted curve for the singular rise of the cutoff TMSS frequency in Fig.3.

The asymptotic form of Eq.(29) can also be theoretically confirmed. Butler (1982) showed analytically that, for the TM mode, a thin longitudinal strip is equivalent to a small cylinder with a radius which is 1/4 of the width of the strip. This result can also be inferred by complex analysis. Near the origin, the Helmholtz equation Eq.(1) becomes the Laplace equation. Conformal mapping, without disturbing conditions in the far field, shows that a circle can be transformed to a slit of width 4 times its radius (e.g. Churchill and Brown 1984). Now from Wang (1998) the fundamental frequency in an annular region with a small core of radius ε is Eq.(26), with

$$k_1 = \frac{\pi Y_0(k_0)}{2J_1(k_0)} = 1.54288 \tag{30}$$

From Butler (1982) $\varepsilon = 2b/4 = b/2$ since 2*b* is the strip width. Eq.(27) then yields

$$\delta = \frac{1}{|\ln \varepsilon|} = \frac{1}{|\ln b - \ln 2|} = \frac{1}{|\ln b(1 - \ln 2 / \ln b)|}$$
$$= \frac{1}{|\ln b|(1 + \ln 2 / |\ln b|)} = \frac{1}{|\ln b|} + O\left(\frac{1}{|\ln b|^2}\right) \quad (31)$$

Thus the analytical asymptotic frequency from Eqs.(26,30,31) is

$$k = 2.4048 + \frac{1.54288}{|\ln b|} + \cdots \quad (32)$$

Our numerical mode-matching method yields Eq.(29), which differs from the analytical result Eq.(32) by less than 0.2% in k_1!

Next we look at the sudden drop in frequency for *b* close to one, for the cutoff TESA mode of the slot line (Fig.2). In order to determine its singular properties, we need to compare with an exact solution similar to the above TMSS case. Since the TESA mode has a small zero- value strip near the center, the boundary conditions are topologically similar to an annular region with zero derivative on the outer boundary and zero value on the inner boundary. The exact solution is Eq.(33)

$$w = J_0'(k)Y_0(kr) - Y_0'(k)J_0(kr) \quad (33)$$

Using the boundary condition, Eq.(33) gives the characteristic equation

$$J_0'(k)Y_0(ka) - Y_0'(k)J_0(ka) = 0 \quad (34)$$

where a=1-b<<1. Let

$$k = \delta(a)k_1 + o(\delta) \quad (35)$$

where $\delta(a)$ is a guage function to be determined. Eq.(34) is then asymptotically expanded for small k and small a . After some work, the leading terms from Eq.(35) are

$$\frac{k_1}{2}\delta(a)\ln a + \frac{1}{k_1\delta(a)} = 0 \quad (36)$$

Balancing Eq.(36) yields

$$k_1 = \sqrt{2}, \quad \delta(a) = \frac{1}{|\ln a|^{1/2}} \quad (37)$$

Although our small strip is not the same as a small circle, the form of the singularity is still governed by Eqs. (35), albeit with a different coefficient k_1 as in Eq.(37). We expect for the slot line the TESA cutoff frequency is also proportional to the inverse square root of logarithmic (1-*b*). Using data for *b*=0.9, 0.95, 0.99 we find Eq.(38)

$$k = \frac{1.42}{\left|\ln(1-b)\right|^{1/2}} \tag{38}$$

This approximation is plotted in Fig 2 as the dotted curve.

Similar arguments show the TESA cutoff frequency of the strip line (Fig.3) has the same asymptotic behavior. We find Eq.(39)

$$k = \frac{1.31}{\left|\ln(1-b)\right|^{1/2}} \tag{39}$$

Fig. 3 shows the higher TE modes also have singular drop when *b* is close to 1. However, the drops stops at finite frequency values. The form is found to be similar to Eqs. (26,27). For the first TEAA mode we find Eq.(40)

$$k = 1.8412 + \frac{1.30}{\left|\ln(1-b)\right|} \tag{40}$$

For the second TESA mode we obtain Eq.(41)

$$k = 3.0542 + \frac{0.99}{\left|\ln(1-b)\right|} \tag{41}$$

For the second TEAA mode the asymptotic form is Eq.(42)

$$k = 4.2012 + \frac{0.97}{\left|\ln(1-b)\right|} \tag{42}$$

These approximations are also shown in Fig. 3.

4. THE MODE SHAPES

Of interest are the changes in mode shapes which have not been reported previously. The cutoff TM modes of the slot line are shown in Fig. 5 for various fin length *b*. Note that as the fin length is increased (slot width decreased) the original circular TM mode is pinched into two semi-circular modes which have a higher frequency. Fig. 6 shows the first five TM modes for the same fin length *b*=0.5. The first mode is the fundamental TMSS mode. In the second mode (TMSA) and the fourth mode (TMAA) the fins lie on the nodal diameter, and have no effect on

the mode shape. The pinching fins of the third mode (TMAS) and the fifth mode (TMSS), being added constraints, raise the frequency.

Fig. 7 shows the cutoff TE mode (TESA) for the slot line. For TE modes the normal derivative of the wave amplitude is zero on the boundary. When the fins are absent, the cutoff frequency is 1.8412 with one nodal diameter. As the fin lengths increase, they encroaches on the nodal diameter, which can be regarded as a fixed constraint. Thus the frequency decreases. When the fins touch, all constraints are eliminated and we have zero frequency. Fig. 7 however, does not give any insight of the singular decrease in frequency as shown in Fig. 2. Fig. 8 shows the first five TE modes for b=0.5. We see that the second mode (TEAS) and the fourth mode (TESS) the fins are on a symmetry line thus have no effect on the frequencies.

Fig. 9 shows the cutoff TM mode (TMSS) for the strip line. The frequency has a singular rise from the no-strip value of 1.8412 then the strip bisects the circular waveguide into two halves. Fig. 10 shows the first five TM modes for the strip line for b=0.5. The strips in the second mode (TMSA) and the fourth mode (TMAA) lie on the nodal diameter thus have no effect on the frequencies.

Fig.11 shows the cutoff TE mode for the strip line. Similar to the slot line, the strip, with zero normal derivatives of the wave amplitude, negates the constrictive effect of the nodal diameter, thus reduces the frequency. Fig. 12 shows the first five TE frequencies for the strip line for b=0.5. In the second mode (TEAS) and the fourth mode (TESS) the strips are on symmetry lines thus have no effect on the frequencies.

5. DISCUSSIONS

In view of the mode shapes in the previous section, our classification using subscript S (symmetry) and A (anti-symmetry) truly reflects the mode shapes. Previous authors extended the numerical subscripts of the empty circular waveguide to the finned waveguide, e.g. Using TE11 as the fundamental (cutoff) TE mode. However, from Fig. 2 we see that the TE11 of the circular waveguide has two branches, TESA ans TEAS. On the other hand, the first TEAA mode morphs from a circular TE21 mode to a circular TE11 mode. Thus the numerical subscripts lose their original meaning of the number of nodal diameters and nodal circles.

Our method of domain decomposition and mode matching is most suitable for the analyses of slot lines and strip lines. The method is accurate and efficient, especially near the singular regions. Other methods such as finite elements would involve the square of the number of computations, in addition, due to scaling difficulties near the sharp edges, the accuracy of the frequencies near the singularities would be compromised. Similarly the method of singular integrals is also poor near the singularity (Fig.4). The method of Mathieu functions is quite tedious and is exact only if the shield is an ellipse and the fin or strip spans the two foci. For the circular shielded wavegiude, the method of Mathieu functions involve approximation errors.

Comparison of the properties of the slot line and the strip line reveals the following similarities. As the fin length or the strip length increase, in general the TM frequencies increase and the TE frequencies decrease., except for the TMSA, TMAA, TEAS, TESS modes where the frequencies are unchanged. There are also differences. There is a singular increase in the cutoff TMSS mode for the strip line, but none for the slot line. There are singular decreases in the higher TE modes of

the strip line, but no higher modes of the slot line have singular decrease. Most important is our asymptotic analyses near the singularities, where all numerical or semi-numerical methods fail. Our analyses show the singular rise in the cutoff TMSS mode of the strip line is proportional to |ln b|^-1, the singular drops of the cutoff TESA mode of both the slot line and the strip line are proportional to |ln(1-b)|^-1/2, while the singular drop in the higher TE modes of the strip line is proportional to |ln(1-b)|^-1 . The analysis using the analytic results of Butler (1982) particularly supports the singular behaviors revealed in this paper.

Some possible applications of our findings are as follows.

1) Singular rise and singular drop signify the frequencies are sensitive the changes in the lengths of the fins or strip. Thus longitudinal variation of the lengths would serve as a very effective mode control structure.

2) The singular drop in the TE modes lowers especially the cutoff (normalized) frequency. Thus from Eq.(2) the size of the waveguide *R* can be lowered for the same dimensional frequency *f*.

3) The singular drop also widens the bandwidth between adjacent modes, such that mode isolation can be more easily achieved.

6. CONCLUSIONS

The complete frequency spectra for the circularly-shielded slot line and strip line are now determined. As the fin length or strip length increases, some TM modes may have singular logarithmic rise and some TE modes may have singular logarithmic drop in frequency.
Aside from circularly shielded slot lines and fin lines studied in this paper, we expect singular behaviors also exist for waveguides of similar topology. This is because when the gap width of the fins (ridges) is small, locally the geometry is equivalent to a slot line of small gap. On the other hand, small inserts of any shape will be locally equivalent to a small strip line. The following are some recent reports on structures which may have singular behaviors which, if undetected, will seriously affect their performance.

1) Internal fins or ridges are similar to slot lines, for example Qiu et al 2002 (ridges), Zargano et al 2011 (L septa), Liu et al 2012 (ridges). When the gap widths between the fins or ridges become small, there may be singular drop in the TE mode.

2) Small inserts of any shape are similar to strip lines, for example Kononenko and Gandel 2007 (rough circular insert), Chakrabarty et al 2009 (circular), Eom et al 2011 (two strips), Kotsis and Roumeliotis 2013 (circular), Zhou et al 2015 (circular), Wang 2016 (cross). When the nominal sizes of the inserts are small, one may encounter both singular rise in the TM mode and the singular drop in the TE mode.

3) Since the singularities arise from local geometry, their properties will also persist regardless of the shape of the outer shield, whether circular, elliptic, rectangular or otherwise enclosed.

It is hoped that this paper would elicit future theoretical or experimental works in this interesting area.

REFERENCES

[1] Babili, B.T., J.L. Tsalamengas & J.G. Fikioris, 1992. TM and TE modes in cylindrically shielded strip waveguides, *J. Electromag. Waves Appl.* 6:1291-1316.

[2] Bhat, B. & S.K. Koul, 1987. *Analysis, Design and Applications of Fin Lines*. Norwood: Artech House.

[3] Butler, C.M., 1982. The equivalent radius of a narrow conducting strip, *IEEE Trans. Ant. Prop.* AP-30: 755-758.

[4] Chakrabarty, S.B., S.B. Sharma & B.N. Das, 2009. Higher order modes in circular eccentric waveguides, *Electromagnetics* 29:377-383.

[5] Chen, C.W., C.M. Fan, D.L. Young, K. Murugesan & C.C. Tsai. 2005. Eigenanalysis for membranes with stringers using the method of fundamental solutions and domain decomposition, *Comp. Model. Eng. Sci*. 8: 29-44.

[6] Collin, R.E. 1960. *Field Theory of guided waves*. New York: McGraw-Hill.

[7] Edwards, T. 1992. *Foundations for Microstrip Circuit Design*. New York: Wiley.

[8] El-Sherbiny, A.A. 1973. Cutoff wavelengths of ridged, circular and elliptic guides, *IEEE Trans. Microwave Theory Tech.* MTT-21:7-12.

[9] Eom, H.J., J.J. Kim, J.S. Ock, Y.S. Lee, & J.H. Kwon, 2011. Higher-order modes for shielded offset striplines. *IEICE Trans. Comm.* E94-B: 330-333.

[10] Gupta, K.C., R. Garg, I. Bahl & P. Bhartia, 1996 *Microstrip lines and Slotlines*. Boston: Artech House.

[11] Kononenko, O.S., & Y.V. Gandel, 2007. Singular and hypersingular integral equations techniques for gyrotron coaxial resonators with a corrugated insert. *Int. J. Infrared Milli. Waves*, 28: 267-274.

[12] Kotsis, A.D., & J.A. Roumeliotis, 2013. Cutoff wavenumbers of eccentric circular metallic waveguides. *IET Microw. Ant. Prop.* 8: 104-111.

[13] Lee, J.W. & J.T. Chen, 2012. A semi-analytical approach for a nonfocal suspended strip in an elliptical waveguide, *IEEE Trans. Microwave Theory Tech.* MTT-60: 3642-3655.

[14] Liu, J., G. Lin, J. Li & H. Zhong, 2012. Analysis of quadruple corner-cut ridged square waveguide using a scaled boundary finite element method, *Appl. Math. Model*. 36: 4797-4809.

[15] Lord Rayleigh, 1945. *The Theory of Sound*. Vol.1, 2nd Ed. New York: Dover.

[16] McLachlan, N.W. 1955. *Bessel Functions*. London: Oxford.

[17] Omar, A.S. & K.F. Schunemann, 1989. Analysis of waveguides with metal inserts, *IEEE Trans. Microwave Theory Tech*. MTT-37: 1924-1932.

[18] Qiu, D., D.M. Klymyshyn & P. Pramanick, 2002. Ridged waveguide structures with improved fundamental mode cutoff wavelength and bandwidth characteristics. *Int. J. RF and Microwave CAE* 12: 190-197.

[19] Ragheb, H.A. & E. Hassan, 2004. Analysis of a suspended strip in a circular cylindrical waveguide, *ACES J*. 19: 165-169.

[20] Tsalamengas, J.L., I.O. Vardiambasis & J.G. Fikioris, 1993. TE and TM modes in circularly shielded slot waveguides, *IEEE Trans. Microwave Theory Tech.* MTT-41: 966-973.

[21] Wang, C.Y. 1998. On the polygonal membrane with a small core, *J. Sound Vib.* 215: 195-199.

[22] Wang, C.Y., 2016. Determination of TM and TE modes of the circular waveguide with a cross-shaped insert using eigenfunction expansions and domain matching, *J. Electromag. Waves Appl*. 30: 1334-1344.

[23] Yu, L.H. & C.Y. Wang, 2001. Fundamental frequencies of a circular membrane with a centered strip, *J. Sound Vib.* 239: 363-368.

[24] Zargano, G.F., V.V. Zemlyakov, & V.V. Krivopustenko, 2011. Electrodynamic analysis of eigenmodes in a rectangular waveguide with two L-shaped septa, *J. Comm. Tech. Electron*. 56: 259-268.

[25] Zhou, J., M. Chen, R. Zhong, & S. Liu, 2015. Analysis of TM and TE modes in eccentric coaxial lines based on bipolar coordinate system. *ACES J*. 30: 1313-1321.

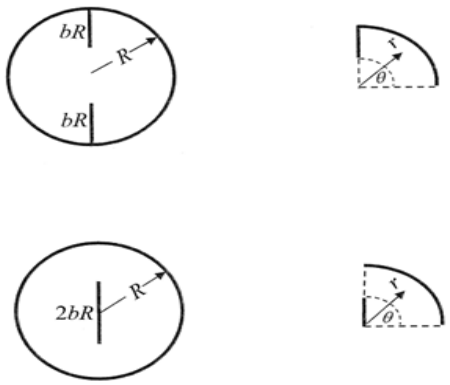

Fig. 1 (a) The slot line in a circular waveguide (b) Representative quadrant (c) The strip line in a circular waveguide (d) Representative quadrant

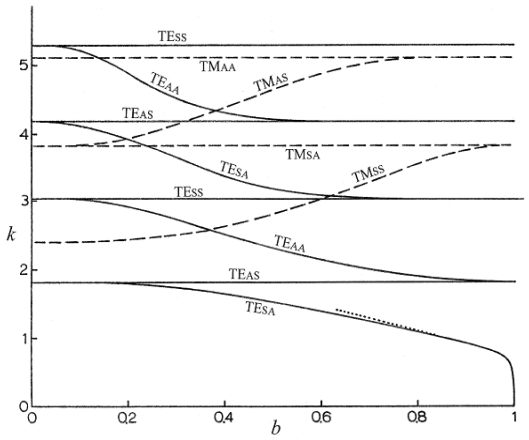

Fig. 2 Frequency versus fin length for the slot line. Solid curves are TE modes, dashed curves are TM modes, dotted curve is the asymptotic approximation Eq.(38).

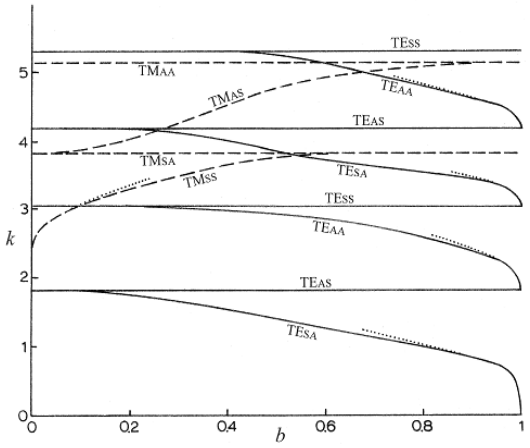

Fig. 3 Frequency versus fin length for the strip line. Solid curves are TE modes, dashed curves are TM modes. Dotted curve for the TMSS mode is from the asymptotic approximation Eq.(29). Dotted curves for the TE modes are from Eqs.(39-41).

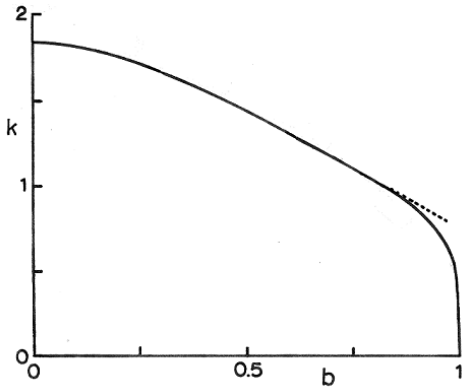

Fig. 4 The fundamental TE Frequency of the strip line. Dashed line is from Babili et al (1992).

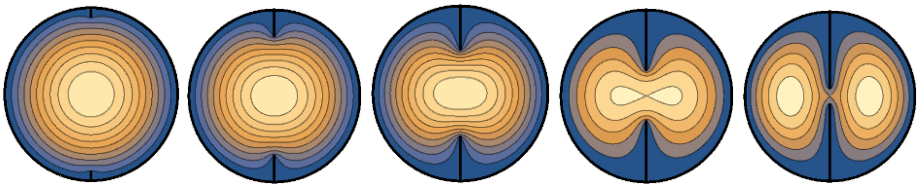

Fig. 5 The cutoff TM mode (TMSS) of the slot line. Values (*b*,*k*) from left: (0.1, 2.415), 0.3, 2.528), (0.5, 2.800), (0.7, 3.290), (0.9, 3.768).

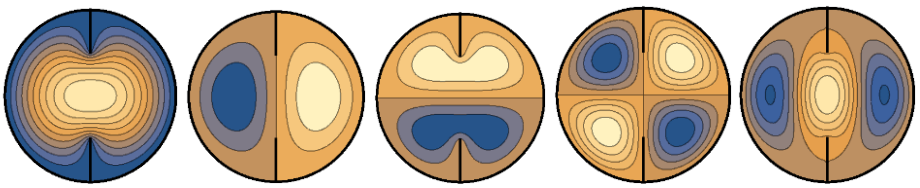

Fig. 6 First five TM modes of the slot line (*b*=0.5). From left: TMSS (*k*=2.800), TMSA (3.832),TMAS (4.671), TMAA (5.136), TMSS (5.444).

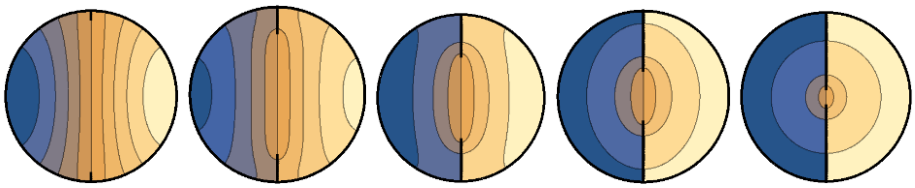

Fig. 7 The cutoff TE mode (TESA) of the slot line. Values (*b*,*k*) from left: (0.1, 1.831), 0.3, 1.737), (0.5, 1.525), (0.7, 1.248), (0.9, 0.928).

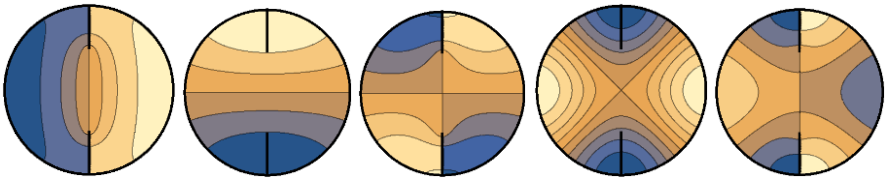

Fig. 8 First five TE modes of the slot line (*b*=0.5). From left: TESA (*k*=1.525), TEAS (1.841),TEAA (2.351), TESS (3.054), TESA (3.202).

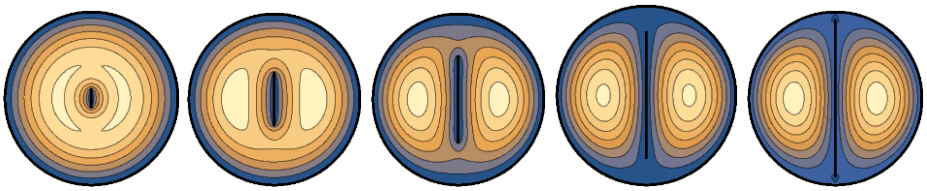

Fig. 9 The cutoff TM mode (TMSS) of the strip line. Values (*b*,*k*) from left: (0.1, 3.060), 0.3, 3.196), (0.5, 3.753), (0.7, 3.824), (0.9, 3.832).

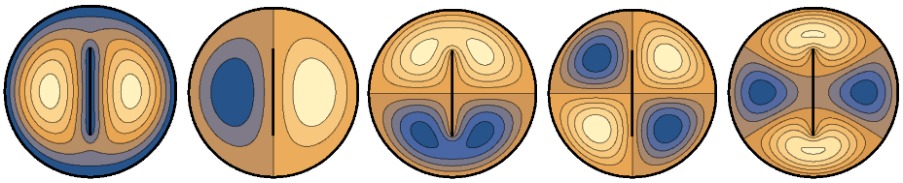

Fig. 10 First five TM modes of the strip line (*b*=0.5). From left: TMSS (*k*=3.753), TMSA (3.832),TMAS (4.798), TMAA (5.136), TMSS (5.681).

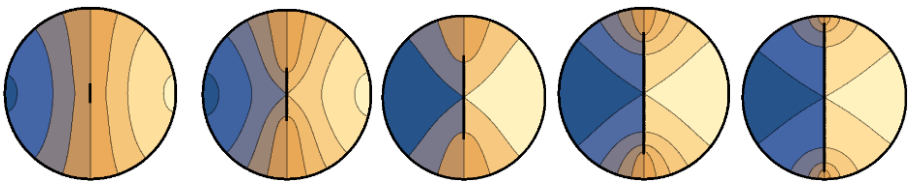

Fig. 11 The cutoff TE mode (TESA) of the strip line. Values (*b*,*k*) from left: (0.1, 1.821), 0.3, 1.667), (0.5, 1.417), (0.7, 1.152), (0.9, 0.861).

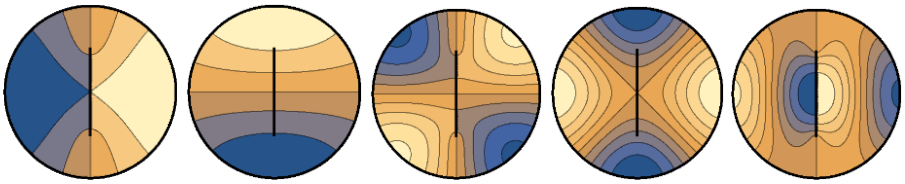

Fig. 12 First five TE modes of the strip line (*b*=0.5). From left: TESA (*k*=1.417), TEAS (1.841),TEAA (2.954), TESS (3.054), TESA (3.851).